Feasible Products in Complex Batch Reactive Distillation

James Chin and Jae W. Lee
Dept. of Chemical Engineering, The City College of New York, New York, NY 10031

Jaehoon Choe
Corporate R&D in LG Chem, Daejeon, South Korea

DOI 10.1002/aic.10795
Published online February 28, 2006 in Wiley InterScience (www.interscience.wiley.com).

A new feasibility evaluation procedure for reactive mixtures is presented, where simple homogeneous reactive batch columns cannot produce pure products. Such columns are not feasible for producing pure products if no node products exist that are reachable by residue curves from the reaction equilibrium manifold. Three alternatives are presented. If an unstable node heterogenous azeotrope decants to an almost-pure product, and *that azeotrope is always reachable from the reaction equilibrium manifold, then a batch reactive rectifier can produce pure products with a decanter. If a homogeneous entrainer allows extractive section profiles to connect the reaction equilibrium manifold to an entrainer-product binary edge, then a homogeneous batch reactive extractive distillation (BRED) column can produce a pure product. If these criteria are not met, then an entrainer that induces an unstable node heterogenous azeotrope between itself and one of the products should be used in a rectifier, a middle-vessel column, or a BRED column.*
 AIChE J, 52: 1790-1805, 2006
Keywords: feasible products, complex batch reactive distillation

Introduction

Reactive distillation has become an attractive process technology in recent years, because of the potential reductions in capital costs, operating costs, and environmental impacts. In particular, reactive distillation can be used to conduct processes that would be prohibitively complicated and unwieldy if handled in a conventional process consisting solely of many single-operation units. This is because of two thermodynamic advantages in carrying out reaction and separation simultaneously rather than sequentially[1-2] (1) phase separation can overcome reaction equilibrium limitations, and (2) chemical reaction can circumvent phase equilibrium limitations, such as azeotropes and distillation boundaries. The Eastman chemical process for producing methyl acetate is a prime example of the benefits of reactive distillation.[3-5] However, it is not a widely applied technology primarily because most of the commercial reactive distillation processes in use today were developed in a trial-and-error manner, with little understanding of how reaction and separation phenomena interact when performed in the same piece of equipment.

Batch production systems are commonly used in the small-scale production of pharmaceuticals, fine chemicals, and specialty chemicals. Batch distillation systems have the advantages of low capital costs, considerable flexibility, the ability to separate multiple components from a single column, being easy to handle, being easy to perform quality control checks on, and usually being able to accept a wide range of feed compositions.

Various studies have been conducted regarding the operating policies and parameters for batch distillation systems[6-8] and batch extractive distillation systems.[9-14] There have been many feasibility studies on nonreactive batch distillation that use residue curve maps (RCMs) to determine feasible product cuts.[10,13,15-18] There have also been studies into the operating

Correspondence concerning this article should be addressed to J. W. Lee at j.lee@ccny.cuny.edu.

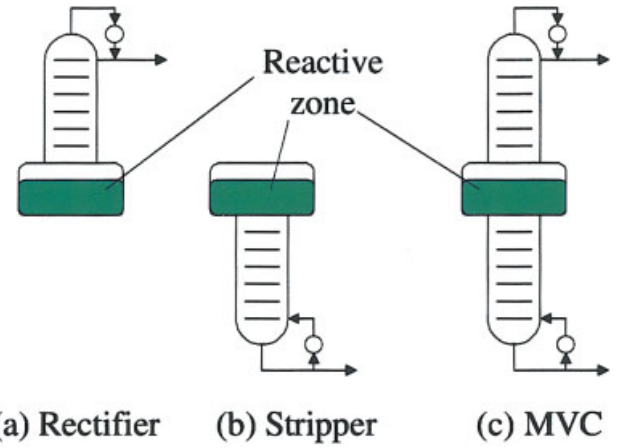

Figure 1. Simple batch column structures.

[Color figure can be viewed in the online issue, which is available at www.interscience.wiley.com.]

policies,[19-20] simulation,[21] and reaction selectivities[22] of batch reactive distillation systems.

However, little attention has been paid to the feasibility study of reactive batch distillation. As a result of this, it has rarely been understood under what conditions simultaneous reaction and V-L separation can lead to the production of pure products. Before performing numerous experiments and simulations, we want to answer this feasibility question by using the relatively simple information of equilibrium data. In our previous work,[23] we determined the following thermodynamic feasibility criteria for simple batch-reactive distillation with reactions of the form $aK + bI \leftrightarrow cL + dH$, or $bI \leftrightarrow cL + dH$:

1. With an unstable node (UN) product that is reachable from the entire reaction equilibrium curve by simple distillation, a batch rectifier with a reactive pot can produce pure products regardless of the number of azeotropes or their dynamic properties. A symmetric result is obtained in a batch stripper with a stable node (SN).

2. If the products are an UN and a SN and share the same distillation region as a part of the reaction equilibrium curve, then pure products can be produced in a batch reactive middle-vessel column (MVC).

Even though the above feasibility criteria apply to a wide range of azeotropic mixtures, there are many phase equilibrium systems that do not meet the criteria listed above for simple batch reactive columns (rectifier, stripper, MVC) that are shown in Figure 1. If there is no node product that is always reachable from the reaction equilibrium curve, then pure products cannot be produced in rectifiers, strippers, or MVC columns. This can happen under any one of the following circumstances: (1) if both products are nodes of the same type (both unstable or both stable), (2) if one of the products is a saddle and a distillation boundary separates the products, and (3) if both products are saddles with or without bounded distillation regions.

In this work, we will first introduce phase equilibrium systems where pure products cannot be produced in the simple batch reactive columns and will show why these columns do not work. To explore the possibility of producing pure products in these systems, we will introduce three alternatives: reactive rectifier with a decanter, homogeneous BRED column, and heterogeneous BRED column (that is, BRED with a decanter). For the two types of BRED, we will introduce the new concept of *projected* upper and lower bounds of reflux ratios with the thermodynamically infeasible region (critical composition region (CCR)[24-25]). We will propose new feasibility criteria by using internal heterogeneity and by using external homogeneous and heterogeneous agents. Some actual reactive systems will be used to highlight our new feasibility studies.

Homogeneous Reactive Rectifiers, Strippers, and Middle-Vessel Columns

In this section, we will examine cases where reactive systems do not meet the feasibility criteria of reactive rectifiers, strippers, or MVCs. A 202-m system (according to Matsuyama

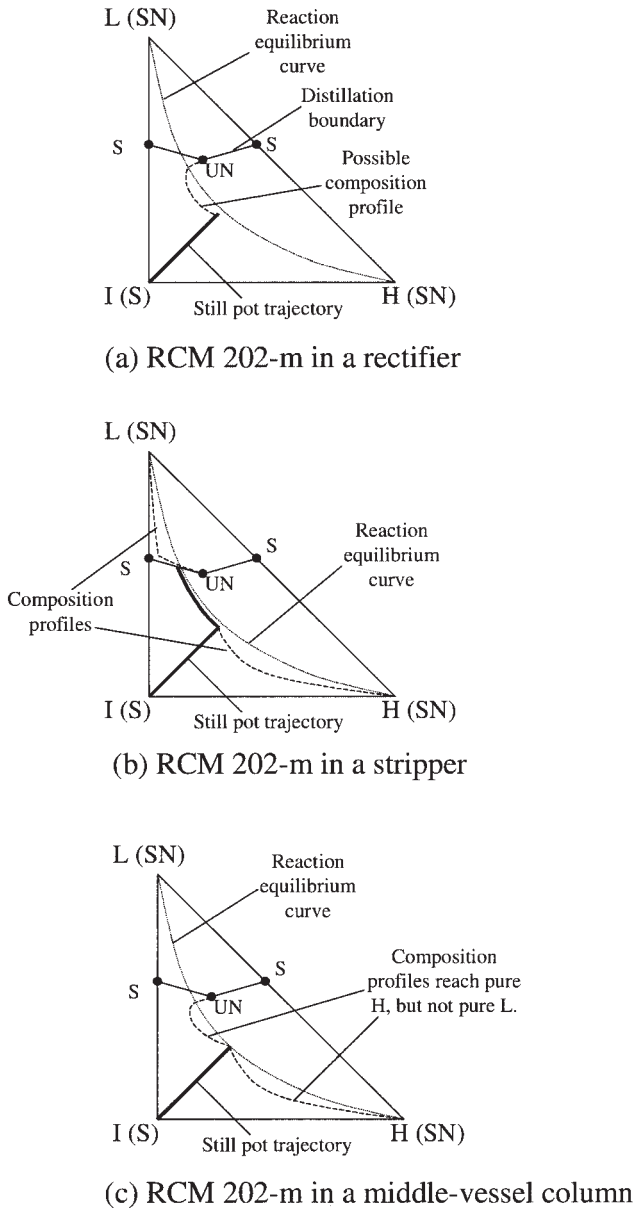

Figure 2. RCM 202-m with reaction $2I \leftrightarrow L + H$.

(a) RCM 202-m in a rectifier. (b) RCM 202-m in a stripper. (c) RCM 202-m in a middle-vessel column.

and Nishimura's classification[26]) is shown in Figure 2. Suppose a reaction of the form bI ↔ cL + dH where product L forms two minimum boiling saddle (S) azeotropes with product H and reactant I, and there is an unstable node (UN) ternary azeotrope. Products H and L are stable nodes (SNs) that are separated by a distillation boundary. This system is not feasible in a batch reactive rectifier because none of the reaction products are UNs as shown in Figure 2a. It is not feasible in a batch reactive stripper because, while the products are both stable nodes, the distillation boundary cuts across the reaction equilibrium curve (regardless of the value of the reaction equilibrium constant). Thus, pure product would be produced at the bottom only until the still pot composition crossed the distillation boundary; thereafter, a different bottoms composition would be obtained (Figure 2b). Batch reactive middle vessel columns cannot produce pure products as the products are separated by a distillation boundary and column profiles cannot lead to both product vertices from any still pot composition (Figure 2c).

A 222-m system is shown in Figure 3a. Here, the node products are separated by a distillation boundary. This system is not feasible in a batch reactive rectifier because none of the reaction products are UNs. It is not feasible in a batch reactive stripper because the distillation boundary cuts across the reaction equilibrium curve, so pure product H would only be produced until the still pot composition crossed the distillation boundary. It is not feasible in a batch reactive MVC because the products are separated by a distillation boundary and column profiles cannot lead to both product vertices from one still pot composition.

A 313-S system is shown in Figure 3b. Again suppose a reaction of the form bI ↔ cL + dH where products L and H are a UN and an S that are separated by a distillation boundary. This system is not feasible in a batch reactive rectifier because a distillation boundary cuts across the reaction equilibrium curve. It is not feasible in a batch reactive stripper because none of the reaction products are SNs. The system is not feasible in a batch reactive MVC because product H is a saddle.

The ethyl acetate production system is shown in Figure 3c, where both of the products are saddles with three binary azeotropes and one ternary azeotrope. The reaction is acetic acid (AC) + ethanol (ETOH) ↔ ethyl acetate (EtAc) + water (W). The only UN is the ethanol-ethyl acetate-water ternary azeotrope and the only stable node is pure acetic acid. This system is not feasible in a batch reactive rectifier, stripper, or middle vessel column because both of the reaction products (EtAc and W) are saddles.

In all four examples, the thermodynamic feasibility criteria are not met in the simple batch reactive columns in Figure 1. To investigate the possibility of producing pure products with these phase equilibrium systems, we propose in the next section a general feasibility evaluation algorithm where different column structures or inert entrainers should be introduced.

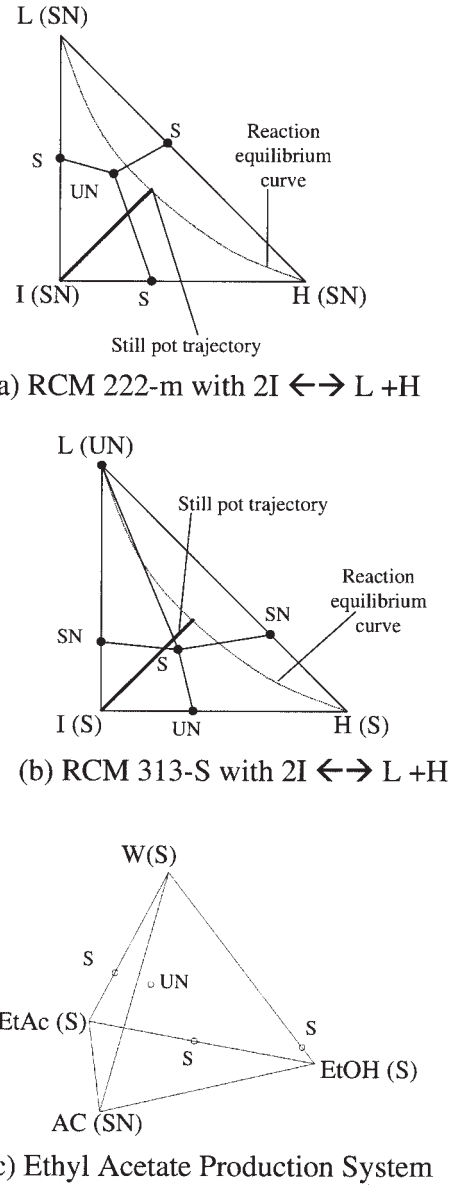

Figure 3: RCMSs where pure products cannot be produced in homogeneous simple batch distillation column.

(a) RCM 222-m with 2I ↔ L +H. (b) RCM 313-S with 2I → L +H. (c) Ethyl acetate production system.

Feasibility Evaluation Algorithm

For a single-reaction system, Figure 4 summarizes which of the column structures considered can be used to produce pure products. The overall algorithm is as follows:

Step 1: Determine if the pure products can be feasibly produced in any of the simple columns (batch rectifier, stripper, or MVC) without decanter. If reaction equilibrium allows node products to be connected to the still pot composition by residue curves or distillation curves, then the rectifier/stripper/MVC can feasibly produce pure products. If feasible, then no further steps in this algorithm need be performed.

Step 2: If the system does not meet the criteria of Step #1, then determine if pure products can be produced with the addition of a decanter. If the system is not feasible in any of the simple columns due to saddle products or distillation boundaries, then check to see if any heterogeneous azeotrope exists in the mixture. If one does exist, then it may be possible to use a batch reactive rectifier *with a decanter* to isolate the heterogenous azeotrope and then separate the azeotrope into

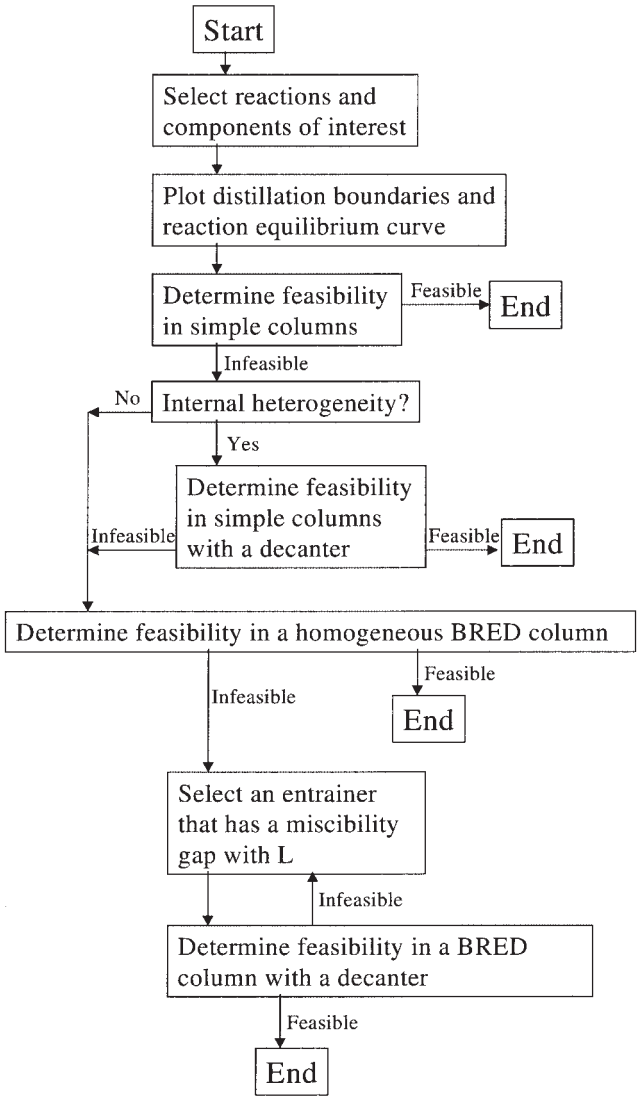

Figure 4. Feasibility evaluation algorithm for complex batch reactive distillation.

two liquid phases containing at least one product. This azeotrope should be an unstable node that is reachable from the reaction equilibrium curve.

Step 3: If the system does not meet the criteria of Steps 1 or 2, then determine if it is feasible in a BRED system with a homogeneous entrainer. Here, we should determine the critical composition region (CCR) and upper and lower bounds of reflux ratios as will be described in the Section of Homogeneous Batch Reactive Extractive Distillation. In short, if the CCR blocks the path of the column profiles or pot trajectories, then the system is thermodynamically infeasible in a homogeneous BRED system under that entrainer. If the CCR does not cover the desired binary edge of light product and heavy entrainer, then perform the upper and lower bound calculations to find feasible ratios of entrainer flow to distillate flow. The column composition profiles and the still pot trajectory must always be in the region where the upper/lower bounds allow the column profiles to isolate a pure product.

Step 4: If the system does not meet the criteria of Steps 1, 2, or 3, then determine if it is feasible in the presence of an external entrainer that forms a liquid-liquid split with one of the existing components. If the system is not feasible under any homogeneous entrainer, then see if it is feasible under a heterogeneous entrainer (specifically, an entrainer that shares a heterogeneous unstable node azeotrope with one of the products). Then see if a batch reactive rectifier or a BRED column or an MVC can isolate the heterogeneous azeotrope. If so, then a decanter can separate the azeotrope into pure products (or into compositions that make downstream purification easy).

Reactive Rectifier with a Decanter for 222-m system

Diisopropyl ether (DIPE) is produced by the dehydration of isopropyl alcohol (IPOH). The equilibrium-governed reaction is 2IPOH ↔ DIPE + W. The phase equilibrium behavior is that of a 222-m system with a liquid-liquid split between DIPE and water (W) as shown in Figure 5 (using NRTL binary parameters in Aspen Plus[27]: VLE-LIT for IPOH-DIPE & IPOH-W and LLE-ASPEN for DIPE-W). Thus, pure DIPE and W cannot be produced in the homogeneous simple batch columns as already shown in Figure 3a. However, if we take advantage of the large miscibility gap, we can produce almost pure DIPE and water using a rectifier with a decanter as suggested in Step 2 of the Feasibility Evaluation Algorithm. The azeotropes are marked with their boiling point temperatures and dynamic properties and they are connected by distillation boundaries. The reaction equilibrium curve is drawn as a dashed curve going from the water vertex to the DIPE vertex by using information from Aspen Plus ($\ln(Keq) = -3.00561 + 1464/T + 61892.8/T^2$, as fitted by Mathematica[28]). The solid curve going from the IPOH vertex, to the reaction equilibrium curve, and then to the DIPE vertex is a rigorously simulated still pot trajectory with coupled heat and material balances. Constant reflux policy is adopted with a reflux ratio of 10. Since no reaction occurs on the trays and fast reaction is assumed to take place in the still pot, pseudo-steady

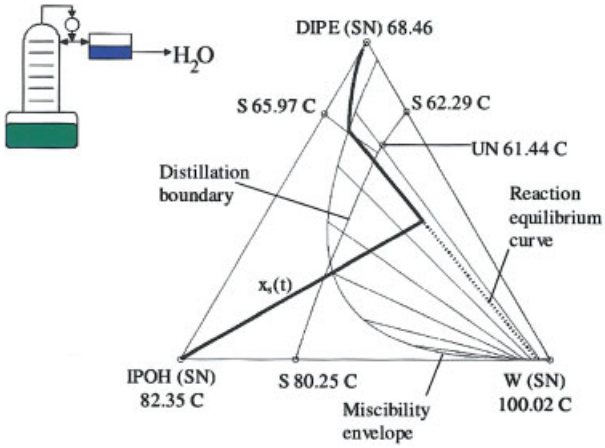

Figure 5. Simulation result of one of 222-m systems: 2IPOH ↔ DIPE+W (10 rectifying stages and 97.4% conversion of IPOH).

[Color figure can be viewed in the online issue, which is available at www.interscience.wiley.com.]

state is assumed for these trays.[19] The detailed simulation model is given in the Appendix.

The features of interest to us in the DIPE system are that the unstable node ternary azeotrope is inside the miscibility gap *and* that one end of the liquid-liquid tie line going through this azeotrope falls near the water vertex. So, when the azeotropic composition is condensed, it splits into two liquid phases: an aqueous phase of relatively pure water (97.27 mol %), and an organic phase that is 78.69 mol % DIPE, 13.37 mol % IPOH, and 7.93 mol % water. *The ternary azeotrope is the only unstable node in the system, so it is always possible to use a rectifier to produce this azeotrope, and then use a decanter to remove a portion of the aqueous phase; the organic phase is completely refluxed.* Thus, we have the same overall effect as a batch reactive rectifier in a feasible homogeneous system: the reaction is driven forward by the continuous removal of one product (water) while the other pure product (DIPE) remains in the pot.

Generalization of Feasibility Criteria in Reactive Rectifier or MVC with a Decanter

Listed in Figures 6 and 7 are the ternary RCMs (as classified in the literature[26]), where the simple homogeneous batch distillation columns shown in Figure 1 cannot lead to the production of pure products with reactions of the form bI $\leftrightarrow$ cL +dH or aL+bI$\leftrightarrow$ cH because distillation boundaries or both saddle products prevent simple distillation from reaching pure product vertices. However, with a decanter in a batch reactive rectifier, we can produce pure products *if the unstable node azeotrope is heterogeneous, reachable from any point in a reaction equilibrium manifold by simple distillation, and the liquid-liquid split from the azeotrope can lead to a pure product vertex.*

The RCMs in Figures 6a-c can have these important features. For example, let's take RCM-021. Reactant I converts to products L and H (bI $\leftrightarrow$ cL +dH) in the reactive still of the rectifier and simple distillation in the column section can lead to an UN heterogeneous azeotrope at the top. This azeotrope is split into the pure L and the L-H mixture in the top decanter. The L is withdrawn as a top product, and the L-H mixture is recycled to the column. The continuous removal of product L forces the reactive still composition trajectory to lie within the forward reaction region. Then, reactant I will be consumed and finally heavy product H will be left in the still pot. Even though all of the other RCMs in Figure 6a have different numbers and types (UN, SN, or S) of azeotropes, the UN azeotrope is reachable from any distillation region or reaction equilibrium curve. Thus, we can isolate pure product L at the top decanter from that azeotrope.

Several systems in Figure 6b have two heterogeneous azeotropes (UNs). These RCMs can also lead to the production of pure product L at the top decanter if the L-H UN azeotrope shares the same distillation region with the reaction equilibrium curve and is reachable from the reaction equilibrium curve by simple distillation. If UN heterogeneous azeotropes exist only on the I-H edges as shown in Figure 6c, then pure product H can be withdrawn at the top decanter.

With a reactive rectifier-decanter, most of the RCMs in Figure 6 can also lead to the production of pure product H with the reaction of aL + bI $\leftrightarrow$ cH. However, the H product cannot be isolated at the top decanter when the UN heterogeneous

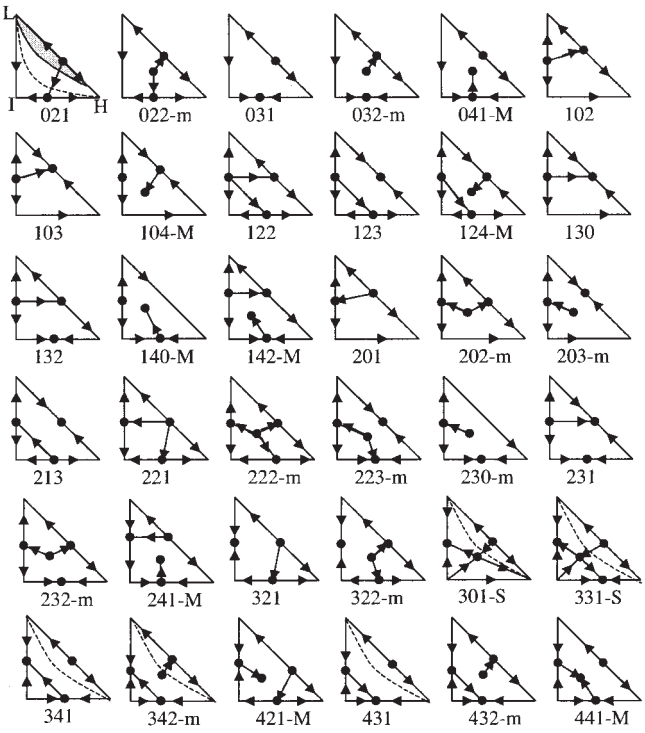

(a) RCMs for possible production of product L at the top decanter.

(b) RCMs for possible two UNs of heterogeneous azeotropes.

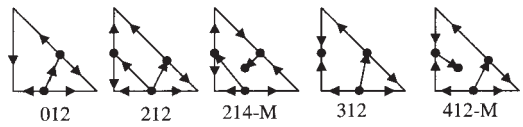

(c) RCMs for possible production of product H at the top decanter.

Figure 6. Feasible RCMs producing pure products with bI $\rightarrow$ cL+dH in a reactive rectifier — decanter.

Dotted lines are reaction equilibrium curves and a hatched region is a possible L-L split. (a) RCMs for possible production of product L at the top decanter. (b) RCMs for possible two UNs of heterogeneous azeotropes, and (c) RCMs for possible production of product H at the top decanter.

azeotrope exists only between L and I as shown in Figure 7a. In this case, a single product H cannot be produced as a pure form in a reactive rectifier-decanter. In contrast, Figure 7b shows the RCMs where reaction bI $\leftrightarrow$ cL +dH cannot lead to production of pure L and H in a reactive rectifier-decanter. This is because the only UN azeotrope between I and H is not accessible from the reaction equilibrium curve due to distillation boundaries. However, with the composition reaction of aL + bI $\leftrightarrow$ cH, pure product H can be isolated at the top decanter as long as the reaction causes the still composition to move to any distillation region where the UN heterogeneous I-H azeotrope is accessible.

In the same sense, a quaternary system with an internal heterogeneity (aK+bI $\leftrightarrow$ cL+dH) will be feasible if a misci-

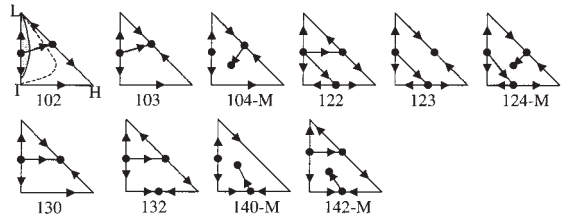

(a) Infeasible RCMs for production of product H at the top decanter with aL+ bI ↔ cH.

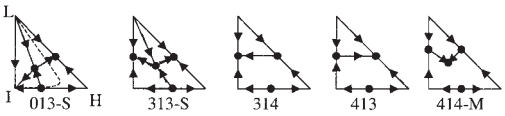

(b)Feasible RCMs with aL+ bI ↔ cH but infeasible RCMs with bI ↔ cL+ dH.

Figure 7. Infeasible and feasible RCMs for producing pure product H with aL+ Bi ↔ cH in a reactive rectifier — decanter.

Dotted lines are reaction equilibrium curves and a hatched region is a possible L-L split. (a) Infeasible RCMs for production of product H at the top decanter with aL+ bI ↔ cH. (b) Feasible RCMs with aL+ bI ↔ cH, but infeasible RCMs with bI ↔ cL+ dH.

bility gap exists between a product and any other component, if that gap has an unstable node heterogenous azeotrope in it, if that azeotrope has a sharp split with that product, and if that azeotrope is always reachable from the reaction equilibrium surface by simple distillation like the butyl acetate production system.[19]

Homogeneous Batch Reactive Extractive Distillation

We now consider homogeneous batch reactive extractive distillation (BRED) systems that do not split into two-liquid phases as shown in Step 3 of the Feasibility Evaluation Algorithm. A BRED column is similar in construction to a batch reactive rectifier, with the exception that an extractive agent is fed into the column on one of the trays above the still pot as shown in Figure 8. We have developed design techniques for extractive sections in double-feed continuous columns[24-25,29]. These techniques are concerned with a column profile approaching the extractive feed stage from below, so a balance

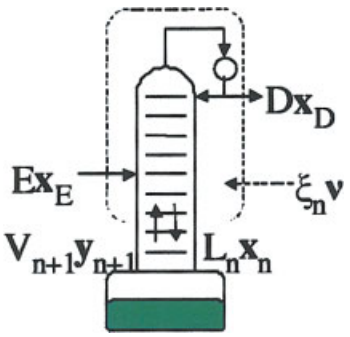

Figure 8. Batch reactive extractive distillation column (BRED).

[Color figure can be viewed in the online issue, which is available at www.interscience.wiley.com.]

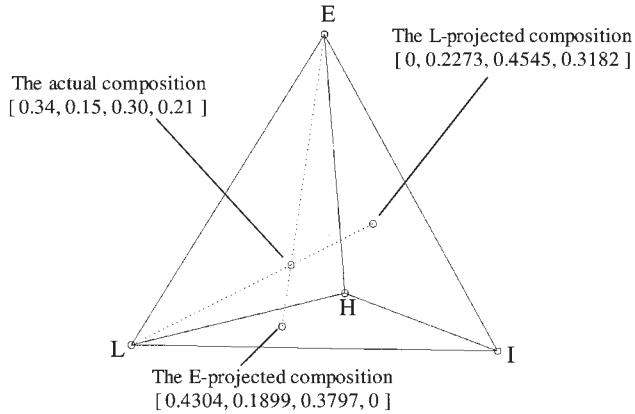

Figure 9. Projection of a quaternary composition to two ternary triangles.

envelope is drawn around the column from the condenser down to an arbitrary tray in the extractive section. As such an envelope can be drawn in both batch and continuous cases, the techniques apply identically to the extractive section of a BRED column. Different from this previous work,[24-25,29] we need to define the projected upper and lower bounds of reflux ratios since we will analyze nonreactive trays with four components in Figure 8. First, we revisit projected compositions and the critical composition region, and then derive the projected upper and lower bounds of reflux ratios.

Projected compositions

To obtain a projected composition, one of the pure components of the system is excluded from the composition vector and the remaining components are renormalized to a sum of 1. Geometrically, this means that in composition space, a line is drawn from the point-of-projection (POP), through the composition to be projected, to the boundary of composition space opposite the POP. The POP is the pure component vertex of the component being excluded from the composition vector. A projected fraction (for either the liquid or the vapor) is defined as

$$\tilde{x}_{i,POP} = \frac{x_i}{(1 - x_{POP})} = \frac{x_i}{\sum_{j=1(\neq POP)}^{N} x_j} \tag{1}$$

$$\tilde{y}_{i,POP} = \frac{y_i}{(1 - y_{POP})} = \frac{y_i}{\sum_{j=1(\neq POP)}^{N} y_j} \tag{2}$$

where i is any component *not* being used as the POP, $\tilde{x}_{i,POP}$ is the projected mole fraction of component i under a projection by the POP component, x_i is the actual mole fraction of component i, and x_{pop} is the actual mole fraction of the excluded component (that is, the component used as the POP). $\boldsymbol{x}$ refers to liquid mole fractions, and $\boldsymbol{y}$ refers to vapor mole fractions. Both projected liquids and projected vapors will be used to determine critical composition regions[24-25] and new projected lower and upper bounds of reflux ratios in the next sections.

Figure 9 shows two different projections of the same composition, which is a mixture of four components that we shall call L, I, H, and E. The two L and E projections will be used

in the next subsection since these projections clearly tell us whether possible composition profiles can reach the L-E binary edge as we go up to the feed stage.[25]

Feasible directions for composition profiles — critical composition region

We now employ the concept of feasible directions for composition profiles, as determined by the critical composition region[24-25]. Consider the reaction $2I \leftrightarrow L + H$ in the presence of inert entrainer E where L, I, and H are the light-, intermediate-, and heavy-boiling components. Pure product L is a saddle in both the L-I-H and the L-I-H-E systems, and simple batch reactive columns (rectifier, stripper, and MVC) cannot be used to produce pure products. In a homogeneous BRED system, an entrainer is chosen such that L and E do not form a binary minimum boiling azeotrope. Then, a rectifying section can separate the mixture and isolate L in the distillate once the extractive composition profile approaches the L-E edge in the feed stage. For a BRED column to be feasible in a given reaction/phase equilibrium system, the extractive column profiles must be able to reach the L-E edge of composition space from any possible still pot composition. However, there is a region in composition space where phase equilibrium does not allow composition profiles to approach the L-E edge. This region is called the critical composition region (CCR),[24-25] and is defined as the region in composition space where, for a given liquid/vapor pair in phase equilibrium, the projected fraction of L in the liquid is greater than the projected fraction of L in the vapor (under an E projection) **and** the projected fraction of E in the liquid is greater than the projected fraction of E in the vapor (under an L projection). That is, the CCR is the set of compositions where the inequalities and are both true.[25] Any composition profile entering the CCR cannot reach the L-E edge while moving up the column.[24-25]

The CCR must also not cover the H-E edge of composition space because, toward the end of the reactive distillation, H and E will accumulate in the still pot to the exclusion of L (which is being distilled out) and I (which is being consumed by reaction). Column composition profiles start from the time-dependent still pot composition. Consequently, a column composition profile must be able to go from compositions near the H-E edge (where the final still pot compositions are) to the L-E edge (where the extractive section profiles join with the rectifying section profiles). *So, for a system to be feasible, the CCR must not cover either the L-E edge or the H-E edge nor block all paths between the two.* The CCR is based only on equilibrium information, process structure, and the choice of desired compositions (we want to isolate an L-E mixture). This criterion does not employ process operation conditions. It constitutes a necessary, but not sufficient, condition for feasible BRED systems.

We take a 202-m system and assume the use of a homogeneous entrainer. The CCR for this region is plotted in Figure 10a. Note that neither the L-E nor H-E edges are completely covered by the CCR. The CCR for the EtAC production system is shown in Figure 10b. In this system, still pot compositions will move toward the W vertex (or the W-AC binary edge, if an excess of AC is used). The CCR allows composition profiles to approach the EtAC-AC binary edge from the W-AC binary edge. Thus, for both of these systems, we can move to the next

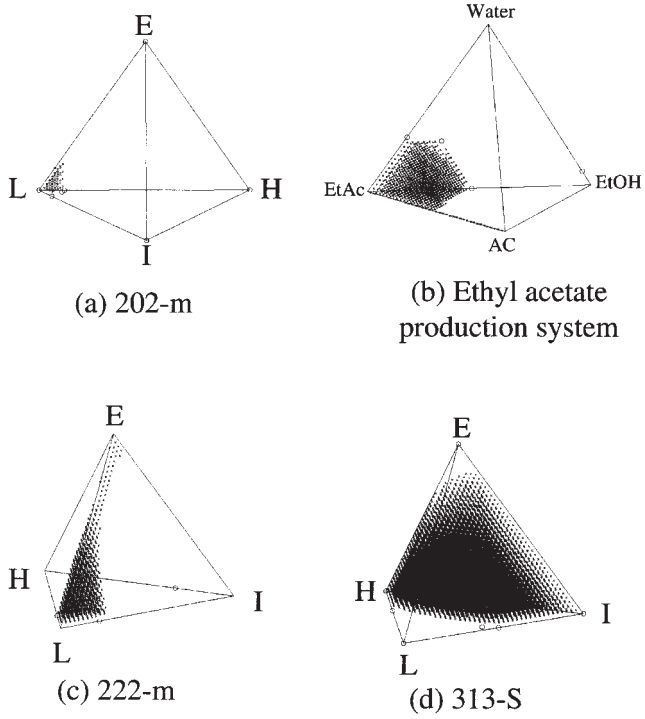

Figure 10 All shaded regions are critical composition regions (CCRs).

(a) 202-m. (b) 222-m. (c) 313-S. (d) Ethyl acetate production system.

step (described in the next section), which is applying the upper/lower bound calculation method. However, in the 222-m and 313-S systems, the CCR covers the L-E and H-E edges (as shown in Figures 10c and 10d), so when still pot trajectories enter the CCR, column profiles are unable to approach the L-E edge.

The CCR was only drawn on the reaction equilibrium surface in previous work.[24-25] This is because our consideration was limited to the reactive trays of a continuous distillation column. The calculation of the CCR does not require this limitation and, in BRED systems, the trays above the reactive pot are assumed to be nonreactive. Thus, for columns with nonreactive trays as in Figure 8, it is necessary to perform the CCR calculations everywhere in composition space using only phase equilibrium data.

Feasible directions for composition profiles — projected upper and lower bounds of the internal reflux ratio

The CCR in the previous sub-section is the thermodynamically infeasible region of a BRED column. Now, in this section, material balance constraints will be imposed for given liquid and vapor compositions to see whether BRED column profiles can reach a desired binary edge between the light product and heavy entrainer vertices.

In previous work,[24-25,29] the feasible regions for column composition profiles were calculated for the nonreactive acetone-methanol-water system and several esterification and etherification systems. This was done by drawing a material balance envelope around the top of the column down to some

arbitrary stage in the extractive section as shown in Figure 8. The material balance equations are

$$E + V_{n+1} = L_n + D - \nu_T \xi \tag{3}$$

$$E\boldsymbol{x}_E + V_{n+1}\boldsymbol{y}_{n+1} = L_n\boldsymbol{x}_n + D\boldsymbol{x}_D - \boldsymbol{\nu}\xi \tag{4}$$

where E and $\boldsymbol{x}_E$ are the molar flow rate and molar composition of the entrainer feed stream, V_{n+1} and $\boldsymbol{y}_{n+1}$ are the molar flow rate and molar composition of the vapor stream leaving stage $n+1$ and entering the balance envelope, L_n, and $\boldsymbol{x}_n$ are the molar flow rate and molar composition of the liquid stream leaving stage n, and leaving the balance envelope, and D and $\boldsymbol{x}_D$ are the molar flow rate and molar composition of the distillate stream. ν_T is the total sum of the stoichiometric coefficients, and $\boldsymbol{\nu}$ is the stoichiometric coefficient vector.

By assuming that this arbitrary stage n was pinched ($\boldsymbol{y}_n = \boldsymbol{y}_{n+1}$ or $\boldsymbol{x}_n = \boldsymbol{x}_{n-1}$), the material balance lines described in Eqs. 3 and 4 become pseudo-balance lines instead. For given phase equilibrium data, the following feasibility condition to approach the L-E edge was derived[25]

$$\frac{L_n}{D} \le \left(\frac{V_n}{E}\frac{E}{D} + \frac{E}{D} + \nu_T \frac{\xi_n}{D} - 1 \right) \tag{5}$$

where the left and right sides are the lower and upper bounds of the internal reflux ratios for arbitrary equilibrated compositions of $\boldsymbol{x}_n$ and $\boldsymbol{y}_n$ at arbitrary stage n. If the upper bound is greater than the lower bound at these arbitrary equilibrated compositions, then the composition profiles passing those compositions can move to the desired binary edge between the light product and the entrainer while going up the column.

With a 3-component system such as the methanol-acetone-water extractive distillation, the arbitrary pseudo-balance lines intersect in a 2-dimensional (2-D) composition space.[29] The same is true of reactive 4-component systems since the liquid compositions of reactive trays are constrained to the reaction equilibrium manifolds[24-25]. However, if the number of components exceeds the number of equilibrium-governed reactions by more than 3 (for example, a 4-component system with no reaction), then the pseudo-balance lines will not intersect. Thus, the pseudo-balance lines generally do not intersect in multicomponent systems. However, the determination of the upper and lower bounds requires having a point-of-intersection. A point-of-intersection can be obtained if the pseudo-balance lines are projected from the full composition space onto 3-component (2-D) subspaces; the projected pseudo-balance lines are then forced to intersect.

The *projected* pseudo-balance equations without reaction are derived from Eq. 4

$$\begin{aligned}\tilde{E}_{POP}\tilde{\boldsymbol{x}}_{E,POP} + \tilde{V}_{n,POP}\tilde{\boldsymbol{y}}_{n,POP} &= \tilde{L}_{n,POP}\tilde{\boldsymbol{x}}_{n,POP} + \tilde{D}_{POP}\tilde{\boldsymbol{x}}_{D,POP} \\ &= (\tilde{E}_{POP} + \tilde{V}_{n,POP})\tilde{\boldsymbol{x}}^*_{POP} = (\tilde{L}_{n,POP} + \tilde{D}_{POP})\tilde{\boldsymbol{x}}^*_{POP}\end{aligned} \tag{6}$$

For the geometrical considerations used in the upper/lower bound approach to make sense, we cannot use a vertex as a POP if that vertex is part of the boundary that we want composition profiles to approach. For example, if one wishes to reach the L-E edge in the extractive section, then any projected subspace to be analyzed must include the L-E edge. Therefore, neither L nor E may be used as a POP to calculate upper and lower bounds. This contrasts with the CCR calculations, where *only* L and E could be used as POPs.

$\tilde{\boldsymbol{x}}^*_{POP}$, the point-of-intersection between the projected pseudo-balance lines, can be determined. From this, the ratios $\tilde{V}_{n,POP}/\tilde{E}_{POP}$ and $\tilde{L}_{n,POP}/\tilde{D}_{POP}$ can be calculated; they are the ratios of the lengths of the segments of the projected pseudo-balance lines. Because we want a feasible projected $\tilde{\boldsymbol{y}}_{n+1}$ to lie further away from the binary edge than $\tilde{\boldsymbol{y}}_n$, we require the projected upper bound (the righthand side of Eq. 7) to be greater than the projected lower bound (the lefthand side of Eq. 7). That is

$$\frac{\tilde{L}_{n,POP}}{\tilde{D}_{POP}} \le \left(\frac{\tilde{V}_{n,POP}}{\tilde{E}_{POP}}\frac{\tilde{E}_{POP}}{\tilde{D}_{POP}} + \frac{\tilde{E}_{POP}}{\tilde{D}_{POP}} - 1 \right) \tag{7}$$

Equality is conserved for pinch points as mathematically proved in the Appendix. Applying the definitions, and to calculate the upper and lower bounds with a given value of E/D, this becomes

$$\frac{\tilde{L}_{n,POP}}{\tilde{D}_{POP}} \le \left(\frac{\tilde{V}_{n,POP}}{\tilde{E}_{POP}}\frac{E}{D}\frac{[1 - x_{E,POP}]}{[1 - x_{D,POP}]} + \frac{E}{D}\frac{[1 - x_{E,POP}]}{[1 - x_{D,POP}]} - 1 \right) \tag{8}$$

Figures 11 and 12 show a pair of pseudo-balance lines for a 4-component system, L, I, H, and E. In both figures, the same liquid and vapor compositions are used, pure E is the entrainer composition, and pure L is the assumed distillate composition. The pseudo-balance lines, themselves, do not intersect, but when projected onto either the L-I-E or the L-H-E faces, the projected pseudo-balance lines do intersect. Figure 11 shows the projection onto L-I-E (H is the POP) and Figure 12 shows the projection onto L-H-E (I is the POP). Then, the lengths of the line segments on both projected pseudo-balance lines can be calculated and, from that, the projected upper and lower bounds can be calculated.

Because it is possible to project the pseudo-balance lines in two different ways, the projected upper and lower bounds are different under the two projections. A column composition profile passing through that liquid composition is feasible if both projected upper bounds are greater than their respective projected lower bounds. As all of the projected upper and lower bounds are functions of the E/D molar flow ratio, the size and shape of the feasibility region will also be a function of the E/D ratio. *For a given E/D ratio, the still pot trajectory and possible column composition profiles should remain inside the feasibility region.*

The feasibility region must cover some part of the L-E edge so that the column profiles may approach it. Since column profiles start at the still pot trajectories and the still pot trajectories will move toward the H-E edge with time, the feasibility region must also cover some part of the H-E edge. *Thus, the feasibility region must cover parts of both the L-E and H-E edges for the column to be feasible at a given E/D ratio.*

Figures 13a and b show the feasibility region for the 202-m system (the same system as shown in Figure 10a under E/D ratios of 5.0 and 23.0, respectively). As the E/D ratio increases,

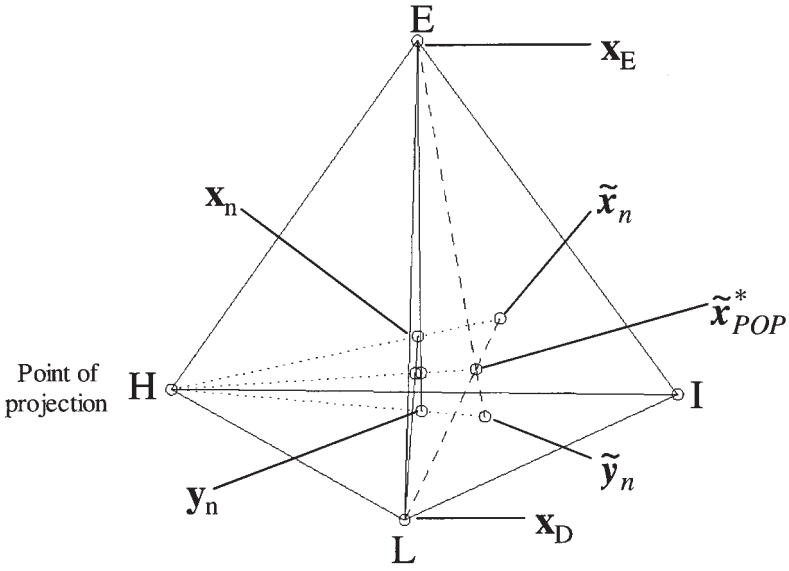

Figure 11. H projection in a quaternary mixture.

the size of the feasibility region also increases, thus making it easier for the extractive section of the column to isolate an L-E mixture at the entrainer feed stage of the column. A comparison of Figure 10a with Figures 13a and b shows that the feasibility region does not intersect the CCR.

Figure 14a shows a rigorously simulated still pot trajectory and column profiles for the 202-m system ($2I \leftrightarrow L + H$, $Keq = K_x K_\gamma = 3.0$) under a homogeneous entrainer. The detailed dynamic model is available in the appendix. The grid of small dots marks the region where the projected upper bounds are greater than the projected lower bounds (E/D = 23.0, the same as in Figure 13b). The still pot composition starts as pure I. It is then allowed to react under total reflux without entrainer to generate L and H in the still pot. Then, we switch to finite reflux and introduce entrainer to the system. Because of the high E/D ratio used, the still pot trajectory quickly travels toward the E vertex of composition space. Although increasing the E/D ratio increases the size of the feasibility region, it does not extend all of the way to the boundary of composition space near the E vertex. So, flooding the column with entrainer causes the still pot composition to leave the feasibility region quickly. Our simulated column was only able to convert 76.1% of the reactant (I) initially charged to the still pot. However, while the still pot composition is in the feasibility region, the

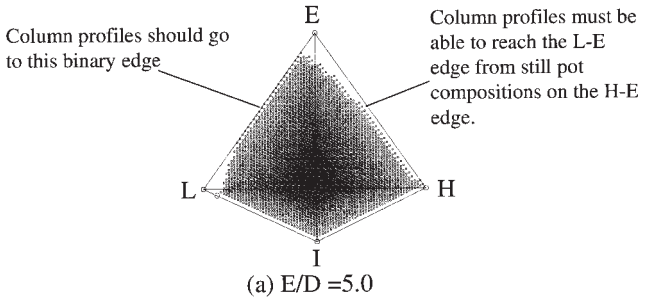

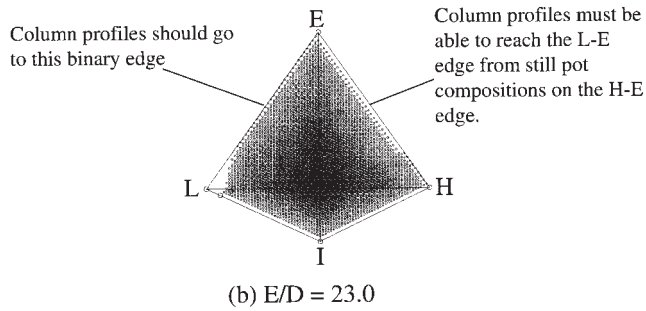

Figure 13. Feasible regions (shaded regions) where upper reflux ratios are greater than lower ratio in RCM 202-m under a homogeneous entrainer.

(a) E/D = 5.0. (b) E/D = 23.0.

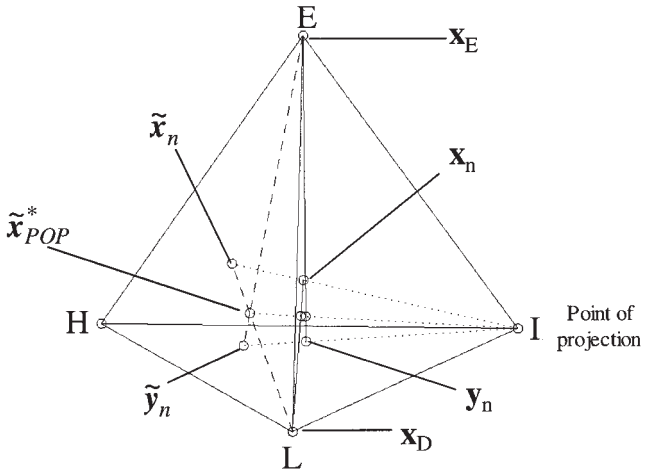

Figure 12. I projection in a quaternary mixture.

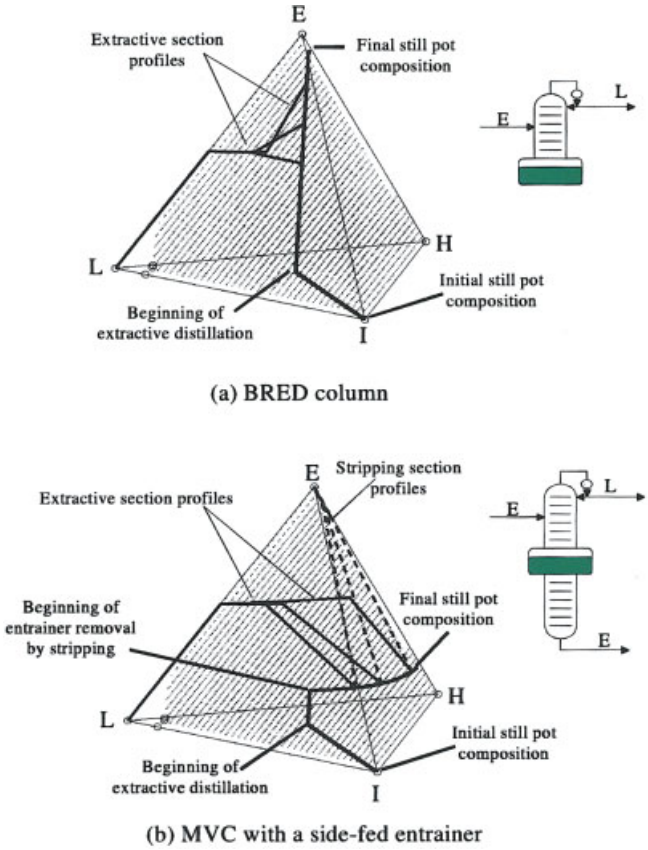

Figure 14. Dynamic simulation results in RCM 202-m with reaction 2I ↔ L+H and nonreactive entrainer E.

(a) BRED column (15 rectifying stages and 50 extractive stages). (b) MVC with a side-fed entrainer (15 rectifying stages, 50 extractive stages, and 9 stripping stages). [Color figure can be viewed in the online issue, which is available at www.interscience.wiley.com.]

extractive profile can reach the L-E edge as shown in Figure 14a and from this we can produce pure product L using a rectifying section.

To prevent the still pot from being flooded by entrainer, we added a stripping column below the still pot to isolate E and remove it from the reaction mixture as shown in Figure 14b; E is the only stable node in this system, so a stripping column can remove E from the system without removing other components. This makes the column a middle-vessel column with a side-fed entrainer. The simulation result for this column is shown in Figure 14b. Here, the still pot composition travels toward the middle of the H-E edge of composition space. This simulated column was able to convert 97.4% of the I charged to the still pot. The slop cut from this batch reactive distillation can be rectified in a nonreactive rectifier to recover small quantities of L-I-H and I-H azeotrope for recycling to the next reactive distillation batch. An additional advantage of using a stripping section is that the E recovered in the bottoms can be recycled immediately back to the entrainer feed stream during the batch reactive distillation; this avoids accumulating a large quantity of E in the still pot and reduces the total amount of E that needs to be present in the system at any given time.

202-m is feasible in a BRED or a MVC BRED column, because the CCR and projected upper/lower bounds allow the extractive section composition profile to approach the L-E binary edge. However, in the 222-m and 313-S systems, the CCR prevents column profiles from approaching the L-E edge as shown Figure 10. The CCR is determined only from thermodynamic information, the column structure, and the choice of top product and entrainer. The upper and lower bound calculations require this same information and the choice of E/D ratio, which is the only process operating variable used in this calculation. Note that the choice of entrainer is important, here. Different entrainers will yield different shapes for the CCR and the feasibility regions. For the 313-S and 222-m systems, we should either exploit an internal heterogeneity like the DIPE system in Figure 5 or create L-L splits by introducing an external heterogeneous entrainer as described in the next section.

Heterogeneous Batch Reactive Distillation with an External Entrainer

If the components of interest do not show a miscibility gap, and the CCR and upper/lower bound reflux ratios tell us that there is no feasible homogeneous entrainer that will make a BRED system feasible, then we should consider the possibility of using a heterogenous entrainer as suggested in Step 4 of the Feasibility Evaluation Algorithm in Figure 4. The main idea is to introduce an external entrainer that shares an unstable node heterogenous azeotrope with one of the reaction products. If internal heterogeneity does not provide a sharp L-L split, an external heterogenous entrainer that causes sharper L-L splits can be used to obtain purer products.

RCM 313-S system with two external entrainers

From Figures 6 and 7, the RCM 313-S system cannot lead to the production of pure products with decomposition reaction (bI ↔ cL + dH), even if there is an internal heterogeneity. If we further assume that there is no such internal heterogeneity, we still may not produce pure products in a homogeneous entrainer in the BRED column since the CCR in the RCM 313-S system covers the E-H edge as shown in Figure 10d.

If an entrainer E can be introduced such that E and L share a heterogenous split by forming a UN azeotrope, then, depending on the size of the miscibility gap, either there is no need to distill L from E or such a distillation would be relatively easy. The rectifying section can isolate the L-E mixture and a decanter can separate the mixture. Here, two external entrainers are used for producing pure products with 2I ↔ L + H (Keq = $K_x K_\gamma$ = 20).

The system shown in Figure 15 is a 313-S system under a light heterogeneous entrainer (E). A sharp miscibility gap exists between L and E and one distillation boundary is present. A reactive rectifier with a decanter can still be used for producing pure products since the UN azeotrope between L and E is shared by both distillation regions and is reachable by simple distillation. Figure 16 shows the dynamic simulation result. The still trajectory starts with reactant I and entrainer E and it ends on the E-H edge. From the still trajectory, all column profiles reach the UN heterogeneous azeotrope at the top stage that is split to light product (L) and L-E mixture. As product L is continuously removed at the top decanter, the reaction equilibrium shifts to the forward reaction and reactant I is com-

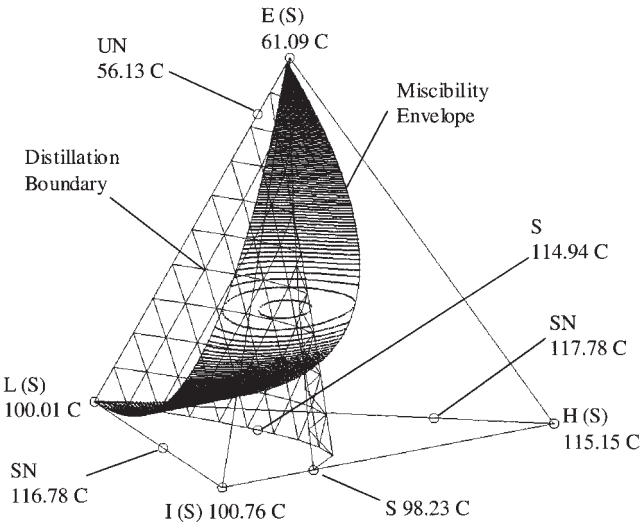

Figure 15. VLLE behavior of 313-S with a light heterogeneous entrainer.

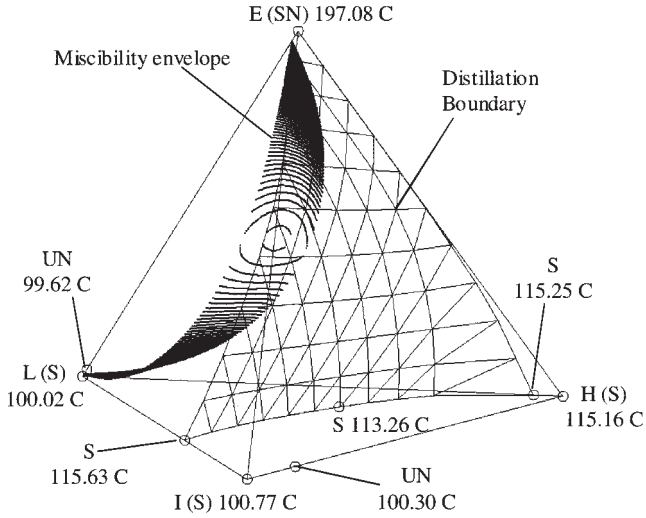

Figure 17. VLLE behavior of 313-S with a heavy heterogeneous entrainer.

pletely consumed as the still trajectory approaches the H-E edge.

If a heavy entrainer is introduced to a 313-S system, then two distillation regions are also formed by a distillation boundary as shown in Figure 17. The quaternary mixture has two UNs: the heterogeneous L-E azeotrope and the homogeneous I-H azeotrope. Pure E is the only stable node in this system. A batch reactive rectifier (that uses an I-E mixture as the initial still charge) will produce the I-H azeotrope instead of the L-E azeotrope if the still pot composition is in the wrong distillation region. Thus, there must be enough entrainer present to keep the still pot composition out of the distillation region containing the I-H azeotrope. In addition, notice that the distillation boundary includes the H-E binary edge. Although the distillation boundary closely follows the E-I-H ternary face at high E fractions, it is possible that a batch reactive rectifier would stop producing the L-E azeotrope as the still pot composition approaches the distillation boundary.

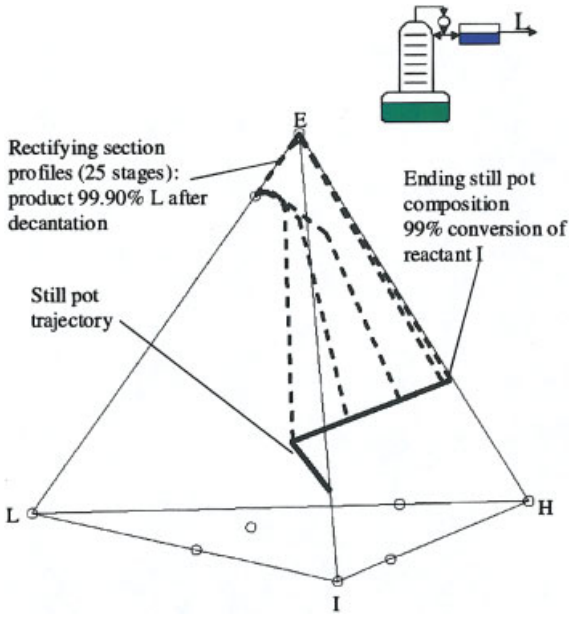

Figure 16. Dynamic simulation result of still trajectory and rectifying section profiles of 313-S with a light heterogeneous entrainer.

[Color figure can be viewed in the online issue, which is available at www.interscience.wiley.com.]

We perform the CCR calculations for this VLLE system to determine if side-feeding this entrainer can circumvent the distillation boundary. In Figure 18a, we see that the CCR does not cover the L-E or H-E edges. We then perform the upper/lower bound calculations to determine the feasible region in Figure 18b. The feasible region includes the L-E and H-E edges. It allows an extractive section profile to cross the distillation boundary, and the rectifying section profile can proceed to the L-E unstable node azeotrope from there. So, a BRED column with side-fed E is used to cross the distillation boundary as shown in Figure 19, and the rectifying section isolates the L-E azeotrope. This azeotrope is then decanted to recover pure L.

The reaction conversion of reactant I is 96.4% in a BRED column-decanter due to the dilution effect of entrainer (E) as seen in Figure 14a. To prevent the flooding of the side-fed entrainer, a middle-vessel column is used to recover the entrainer at the bottom as shown in Figure 20, and it achieves 98% conversion of reactant I. The middle vessel is first charged with an I-E mixture because the feasibility region does not extend to low E fractions. The mixture is allowed to react toward equilibrium without distillation or entrainer. The mixture is then simultaneously distilled under the side-fed entrainer, stripped of entrainer from the still pot, and reacted. The still pot trajectory stays within the feasible region as shown in Figure 20, so column profiles are always able to go to the L-E azeotrope. It is not strictly necessary to use a stripping section to remove pure E from the still pot because the feasible region in Figure 18b includes the E vertex. However, we do not consider it desirable to have E accumulated in the still pot since it is increasingly difficult to distill other components from a reaction mass that is being increasingly diluted by entrainer.

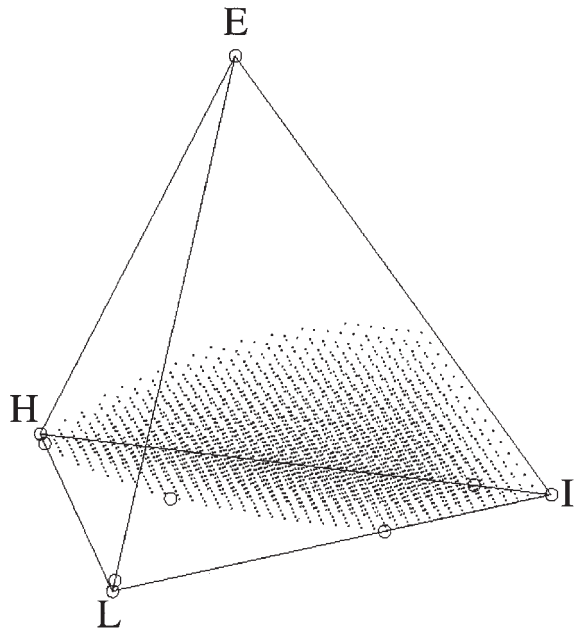

(a) CCR (shaded region)

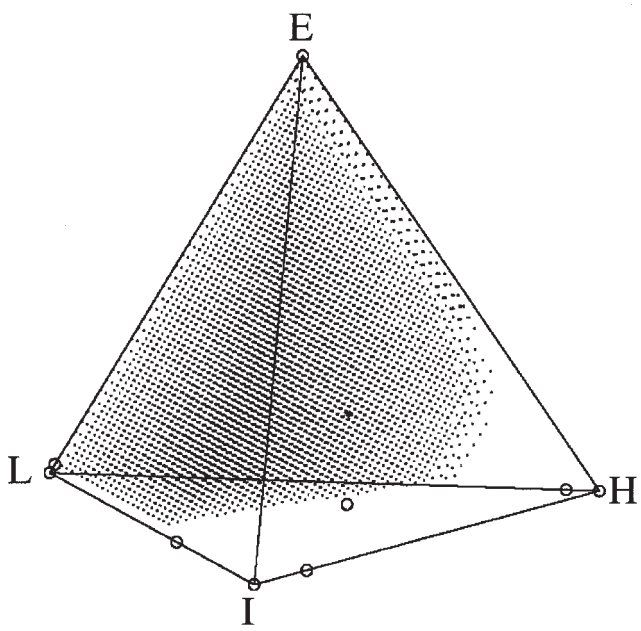

(b) Feasible shaded region with E/D=20

Figure 18. CCR and feasible region in the 313-S system with a heavy entrainer.

(a) CCR (shaded region). (b) Feasible shaded region with E/D = 20.0.

Isopropyl acetate production system

Isopropyl acetate (IPAc) is produced by the esterification of acetic acid (AC) with isopropyl alcohol (IPOH). Water (W) is a byproduct. AC shares no azeotropes with any of the other three components, and is the only stable node in the four-component system. IPOH, IPAc, and W have 3 minimum binary azeotropes and a minimum heterogeneous ternary azeotrope between them that is the only unstable node in the system. Although there are no distillation boundaries, neither the stable node (AC), nor the unstable node (IPOH-IPAc-W azeotrope) is a pure product, so the simple columns will not suffice to produce pure IPAc.

We note that the minimum ternary azeotrope is heterogenous and splits to an organic phase (27.44% IPOH, 45.60% IPAc, 26.96% W) and an aqueous phase (3.21% IPOH, 0.04% IPAc, and 96.75% W). A batch reactive rectifier with a decanter can be used to remove W from the reaction mixture and drive the

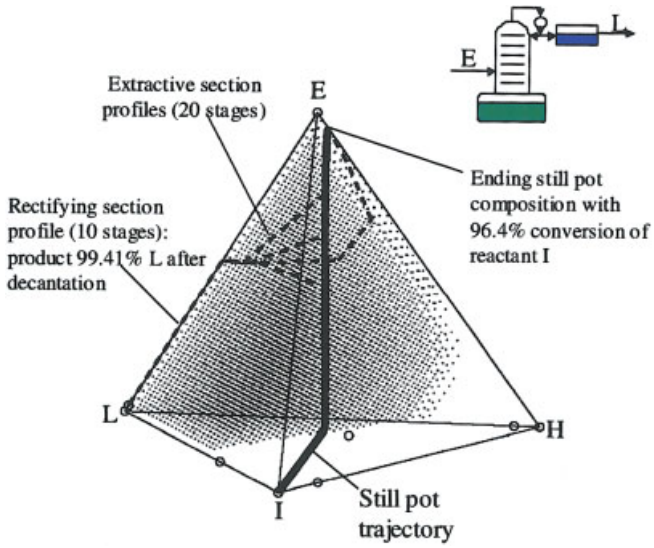

Figure 19. Dynamic simulation result of 313-S in a BRED column-decanter with a heavy heterogeneous entrainer (E/D = 20).

[Color figure can be viewed in the online issue, which is available at www.interscience.wiley.com.]

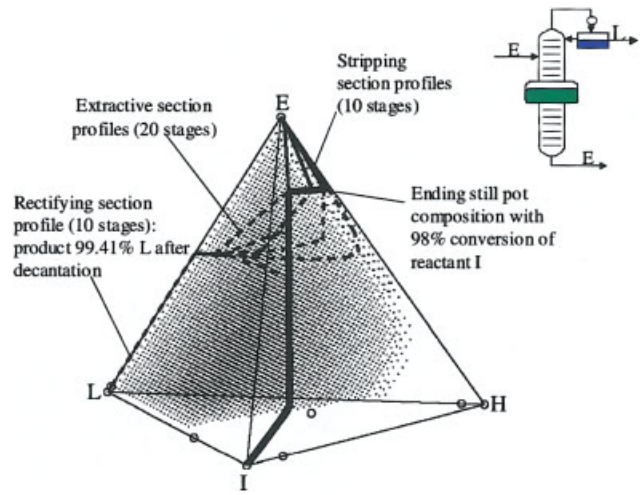

Figure 20. Dynamic simulation result of 313-S in a BRED MVC -decanter with a heavy heterogeneous entrainer (E/D = 20).

[Color figure can be viewed in the online issue, which is available at www.interscience.wiley.com.]

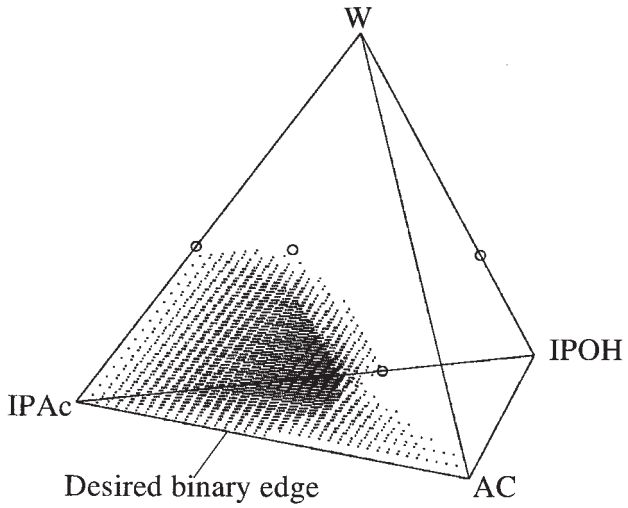

(a) CCR (shaded region)

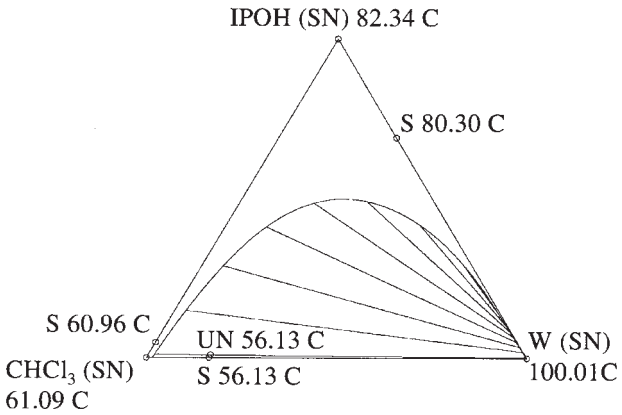

(b) L-L splits between $CHCl_3$ and W

Figure 21. VLLE behavior of the isopropyl acetate production system.

(a) CCR (shaded region). (b) L-L splits between CHCl3 and W.

reaction forward. However, because of the significant presence of IPOH in the aqueous phase, further purification is necessary to recover the reactant IPOH by using an additional nonreactive distillation column.[30] Even if a BRED column is used with a side-feed of AC as an entrainer like the methyl acetate production system, pure IPAc cannot be produced since the CCR covers the whole AC-IPAC binary edge as shown in Figure 21a. Here, if we introduce an external heterogeneous entrainer to a reactive rectifier-decanter such that a sharp split with water is provided, then almost pure water is obtained at the top. The reaction equilibrium constant is 8.7[31] based on the activities of the components in the still pot.

We simulate the case where chloroform ($CHCl_3$) is used as an inert heterogeneous entrainer. The NRTL parameters in Aspen Plus[27] were used for phase equilibrium calculations. Pure AC is the only stable node in the five-component system, but there are two unstable nodes: the IPOH-IPAc-W and the IPOH-W-$CHCl_3$ ternary azeotropes. So, there are two distillation regions according to Rook et al.'s algorithm.[32] One region contains IPOH, IPAC, W, and AC with the azeotropes of IPOH-IPAc-W, IPAc-W, IPOH-W, and IPOH-IPAC. The other distillation region includes all five pure components with the azeotropes of IPOH-W-$CHCl_3$, W-$CHCl_3$, IPOH-CHCl3, IPAC-W, and IPOH-W. The IPOH-W-$CHCl_3$ azeotrope is heterogenous, and the aqueous phase is 0.17% IPOH, 99.73% W, and 0.11% $CHCl_3$ as shown in Figure 21b.

Note that the IPOH-IPAc-W azeotrope lies within the reverse reaction region, and the IPOH-W-$CHCl_3$ azeotrope sits on the reaction equilibrium manifold and is reachable from any point in the forward reaction region by distillation in the column section. Since the initial feed charge containing AC and IPOH with an entrainer ($CHCl_3$) lies within the forward reaction zone, the column section in a rectifier allows its composition profiles to reach the IPOH-W-$CHCl_3$ azeotrope. Once this azeotrope is split to pure water in a decanter and is removed at the top, it will push the reactive still trajectory into the forward reaction zone. Then, reactants IPOH and AC are totally consumed and only IPAc with the entrainer will be left in the still.

The simulation run begins with 42 mol % each of AC and IPOH and 16 mol % $CHCl_3$. The entrainer-projected still pot trajectory is shown in Figure 22. We begin with reaction in the still pot and the column operating at total reflux (so no product is collected) and wait for IPAc and W to accumulate in the still pot. We then switch to finite reflux and begin simultaneous reaction and distillation. The column composition profiles connect the still pot composition to the IPOH-W-$CHCl_3$ azeotrope at all times, so the aqueous phase can be decanted from the condensed azeotrope and water removed at the top. Again, the removal of water from the reaction mixture drives the reaction forward, consuming AC and IPOH and producing more IPAc and W. Eventually, only IPAc and $CHCl_3$ remain in the still pot at the end of the batch reactive distillation. In the same way, we can apply an external heterogeneous entrainer for producing

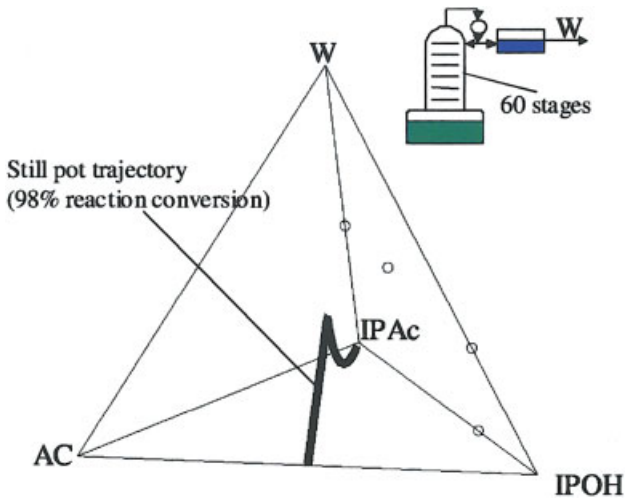

Figure 22. Dynamic simulation result of iso-propyl acetate production in a reactive rectifier — decanter.

Shown is the projected composition space by excluding an entrainer. [Color figure can be viewed in the online issue, which is available at www.interscience.wiley.com.]

pure ethyl acetate (EtAc) in the esterification of acetic acid (AC) with ethyl alcohol (EtOH) in a reactive rectifier-decanter. Adding an external entrainer will also be very helpful for producing pure EtAC since the UN heterogeneous EtOH-EtAc-W azeotrope is *barely* within the L-L miscibility gap.

Conclusions

We have derived feasibility criteria for complex batch-reactive distillation including rectifier-decanter and homogeneous and heterogeneous BRED columns (or middle vessel BRED columns). If none of the products are nodes in RCMs with reaction bI $\leftrightarrow$ cL + dH, or aL +bI$\leftrightarrow$ cH, or aK + bI $\leftrightarrow$ cL + dH, then homogeneous simple rectifiers, strippers, and MVCs cannot produce pure products. Even with a node product being present, these homogeneous batch columns cannot produce pure products if distillation boundaries block column profiles from reaching them. For these cases, we have introduced three alternative ways to produce pure products by using internal or external heterogeneity, and by providing a homogeneous entrainer. If an unstable node heterogenous azeotrope exists between a product and another component (or external entrainer), and it is reachable from the reaction equilibrium manifold using simple or extractive distillation, then a rectifier or a BRED with a decanter can be used to separate a pure product. With no heterogeneity, we can introduce a homogeneous entrainer to a BRED (or middle vessel BRED) column. New projected upper and lower bounds of internal reflux ratios are introduced to analyze nonreactive sections of quaternary distillation in a BRED (or middle vessel BRED) column. This can be extended to multicomponent and multireaction cases to check feasible directions of composition vectors.

Acknowledgments

We are grateful for the support of American Chemical Society - Petroleum Research Fund (ACS-PRF). We also wish to thank Prof. Wolfgang Marquardt at RWTH Aachen for the continued use of his phase equilibrium calculation code, material properties calculation code, and quaternary system visualization program code.

Notation

a, b, c, d = stoichiometric coefficients in ternary and quaternary reactions
D = molar flow rate of the distillate stream
$\tilde{D}_i$ = molar flow rate of the distillate stream under an i projection
E = molar flow rate of side-feed entrainer stream
$\tilde{E}_i$ = molar flow rate of side-feed entrainer stream under an i projection
H, L, K, I = products and reactants in ternary and quaternary reactions
H_S = molar holdup in the still
L_n = molar flow rate of the liquid stream leaving stage n
$\tilde{L}_{n,i}$ = molar flow rate of the liquid stream leaving stage n under an i projection
K_{eq} = reaction equilibrium constant
k_f = forward reaction rate constant, time^{-1}
V_n = molar flow rate of the vapor stream leaving stage n
$\tilde{V}_{n,i}$ = molar flow rate of the vapor stream leaving stage n under an i projection
V_{n+1} = molar flow rate of the vapor stream leaving stage n+1
x_i^* = mole fraction of component i at intersection point of the pseudo-balance lines
$\boldsymbol{x}_D$ = molar composition of the distillate stream
$\tilde{\boldsymbol{x}}_{D,POP}$ = composition of the distillate stream under a POP projection
$x_{D,i}$ = mole fraction of component i in the distillate
$\boldsymbol{x}_E$ = molar composition of the entrainer stream
$x_{E,i}$ = Mole fraction of component i in the entrainer feedstream
$\tilde{\boldsymbol{x}}_{E,POP}$ = composition of the entrainer stream under a POP projection
x_i = mole fraction of component i in an unspecified liquid
$x_{n,i}$ = projected liquid mole fraction of component i under a j projection
$\boldsymbol{x}_n$ = molar composition of the liquid on stage n
$x_{n,i}$ = mole fraction of component i in the liquid leaving stage n
$\tilde{\boldsymbol{x}}_{n,POP}$ = composition of the stage n liquid under a POP projection
$\tilde{\boldsymbol{x}}^*_{POP}$ = composition of the pseudo-balance intersection under a POP projection
x_{POP} = liquid mole fraction of the projecting component. That is x_i where i = POP
$x_{S,i}$ = mole fraction of component i in the still pot
y_i = mole fraction of component i in an unspecified vapor
$\tilde{y}_{i,j}$ = projected vapor mole fraction of component i under a j projection
$y_{n,i}$ = mole fraction of component i in the vapor leaving stage n
y_{POP} = vapor mole fraction of the projecting component. That is, y_i where i = POP
$\boldsymbol{y}_n$ = molar composition of the vapor on stage n
$\tilde{\boldsymbol{y}}_{n,POP}$ = composition of the stage n vapor under a POP projection

Greek letters

$\gamma_{S,i}$ = activity coefficient of component i in the still pot
$\boldsymbol{\delta}_n$ = composition of the cascade different point on stage n
$\delta_{n,i}$ = mole fraction of component i in the cascade different point on stage n
$\boldsymbol{\upsilon}$ = reaction stoichiometry vector
υ_i = stoichiometric coefficient of component i
υ_T = sum of the stoichiometric coefficients
ξ_n = total rate-of-reaction within the material balance envelope of Figure 8

Literature Cited

1. Taylor R, Krishna R. Modelling reactive distillation. *Chem Eng Sci*. 2000;55:5183-5229.
2. Malone MF, Doherty MF. Reactive distillation. *Ind Eng Chem Res*. 2000;39:3953-3957.
3. Agreda VH, Partin LR. Reactive distillation process for the production of methyl acetate. U.S. Patent 4,435,595: 1984.
4. Agreda VH, Partin LR, Heise WH. High purity methyl acetate via reactive distillation. *Chem Eng Prog*. 1990;86(2):40-46.
5. Siirola JJ. An industrial perspective on process synthesis. *AIChE Symp Ser*. 1995;304:222-233.
6. Hasebe S, Noda M, Hashimoto I. Optimal operation policy for multieffect batch distillation system. *Comp Chem Eng*. 1997;21:S1221–S1226.
7. Bonny L. Multicomponent batch distillation: study of operating parameters. *Ind Eng Chem Res*. 1999;38:4759-4768.
8. Kim K, Diwekar UM. Comparing batch column configurations: parametric study involving multiple objectives. *AIChE J*. 2000;46:2475-2488.
9. Lelkes Z, Lang P, Benadda B, Moszlowicz P. Feasibility of extractive distillation in a batch rectifier. *AIChE J*. 1998;44:810-822.
10. Lelkes Z, Lang P, Moszlowicz P, Benadda B, Otterbein M. Batch extractive distillation: the process and the operational policies. *Chem Eng Sci*. 1998;53:1331-1348.
11. Phimister JR, Seider WD. Semicontinuous, middle-vessel extractive distillation. *Comp Chem Eng*. 2000; 24:879-885.
12. Phimister JR, Seider WD. Semicontinuous, middle-vessel distillation of ternary mixtures. *AIChE J*. 2000;46:1508-1520.
13. Safrit BT, Westerberg AW, Diwekar U, Wahnschafft OM. Extending continuous conventional and extractive distillation feasibility insights to batch distillation. *Ind Eng Chem Res*. 1995;34:3257-3264.
14. Safrit BT, Westerberg AW. Improved operation policies for batch extractive distillation columns. *Ind Eng Chem Res*. 1997;36:436-443.
15. Bernot C, Doherty MF, Malone MF. Feasibility and separation sequencing in multicomponent batch distillation. *Chem Eng Sci*. 1991; 46:1311-1326.
16. Lotter SP and Diwekar UM. Shortcut models and feasibility considerations for emerging batch distillation columns. *Ind Chem Eng Res*. 1997;36:760-770.

17. Cheong W, Barton PI. Azeotropic distillation in a middle vessel batch column. 3. Model validation. *Ind Eng Chem Res*. 1999;38:1549-1564.
18. Lang P, Modla G, Benadda B, Lelkes Z. Homoazeotropic distillation of maximum azeotropes in a batch rectifier with continuous entrainer feeding I. Feasibility studies. *Comp Chem Eng*. 2000;24:1665-1671.
19. Venimadhavan G, Malone MF, Doherty MF. A Novel distillate policy for batch reactive distillation with application to the production of butyl acetate. *Ind Chem Eng Res*. 1999;38:714-722.
20. FernholzG, Engell S, Kreul L-U, Gorak A. Optimal operation of a semi-batch reactive distillation column. *Comp Chem Eng*. 2000;24: 1569-1575.
21. Cuille PE, Rekliaitis GV. Dynamic simulation of multicomponent batch rectification with chemical reactions. *Comp Chem Eng.* 1986; 10:389-398.
22. Gadewar SB, Malone MF, Doherty MF. Selectivity targets for batch reactive distillation. *Ind Eng Chem Res*. 2000;39:1565-1575.
23. Guo Z, Ghufran M, Lee JW. Feasible products in batch reactive distillation. *AIChE J.* 2003;49:3161-3172.
24. Lee JW. Feasibility studies on quaternary reactive distillation systems. *Ind Eng Chem Res*. 2002; 41:4632-4642.
25. Chin J, Kattukaran HJ, Lee JW. Generalized feasibility evaluation of equilibrated quaternary reactive distillation systems. *Ind Eng Chem Res*. 2004;43:7092-7102.
26. Matsuyama H, Nishimura H. Topological and thermodynamic classification of ternary vapor-liquid equilibria. *J Chem Engr Japan*. 1977; 10:No. 3;181-187.
27. Aspen Plus 12.1, Aspen Engineering Suite, Aspen Tech; 2005.
28. Mathematica 4.2, Wolfram Research, Inc; 2002.
29. Chin J, Lee JW. Rapid generation of composition profiles for reactive and extractive cascades. *AIChE J.* 2005;51:922-930.
30. Tang YT, Chen YW, Hung SB, Huang HP, Lee MJ, Yu CC. Design of reactive distillations for acetic acid esterification. *AIChE J.* 2005; 51:1683-1699.
31. Lee L, Kuo M. Phase and reaction equilibria of the acetic acid - isopropanol - isopropyl acetate - water system at 760 mmHg. *Fluid Phase Equilibria.* 1996;38:147-165.
32. Rooks RE, Julka V, Doherty MF, Malone MF. Structure of distillation regions for multicomponent azeotropic mixtures. *AIChE J*. 1998;44: 1382-1391.
33. Guo Z, Lee JW. Feasible products in batch reactive extractive distillation. *AIChE J*. 2004;50:1484-1492.
34. Matlab 6.0, Using Matlab. The Math Work, Inc. 2000.

Appendix

Dynamic simulation model

The simulations presented in this article are based on material balance equations derived from references 19, 23, and 33. Their derivation is reproduced here with only minor modifications. We consider a batch column that consists of, at most, a rectifying section, an extractive section, and a stripping section. Pseudo-steady state is adopted for nonreactive column sections since no reaction occurs in the column section and fast reaction is assumed to take place in the still pot. We adopt a relatively simple operating policy as shown in Table 1 for each case.

The time-dependent material balance equations around such a column are

$$\frac{dH_S}{dt} = -D - B + E + \boldsymbol{\nu}_T H_S r \tag{A1}$$

$$\frac{d(H_S x_{S,i})}{dt} = -D x_{D,i} - B x_{B,i} + E x_{E,i} + \boldsymbol{\nu}_i H_s r \tag{A2}$$

A standard middle-vessel column may be considered by setting $E = 0$. A batch reactive stripper may be considered by setting $D = 0$ and $E = 0$. A BRED column may be considered by setting $B = 0$. A batch reactive rectifier may be considered by setting $B = 0$ and $E = 0$. Stage heat balance is coupled with material balance using a special procedure called "mexprops" in the Matlab.[34] For any test run, please contact the corresponding author.

Table A1. Dynamic Simulation Conditions

Operating Policy	Constant Reflux Ratio	Product Withdrawal Rate
Figure 5 (DIPE)	10	
Figure 14 (202-m)	23	
Figure 16 (313-S with a light entrainer)	20	
Figure 19 (313-S with a heavy entrainer)	20	
Figure 20 (313-S with a heavy entrainer in BRED MVC)	20	Proportional to the reactive holdup in the reactive still pot.
Figure 22 (IPA system)	Increasing 80.0, 120.0,and 200.0*.	

*The aqueous reflux ratio increases over time to compensate for decreasing amounts of water in the still pot as distillation proceeds.

We assume a reaction rate of the following form

$$r = k_f \left(\prod_i^{react} (x_{S,i}\gamma_{S,i})^{|\boldsymbol{\nu}_i|} - \prod_i^{prod} (x_{S,i}\gamma_{S,i})^{\boldsymbol{\nu}_i} / K_{eq} \right) \tag{A3}$$

Here, we use a constant reaction rate constant ($k_f = 50$) for all dynamic simulations (assume fast reaction). K_{eq} is given as

$$K_{eq} = \prod_i^{all} (x_{S,i}\gamma_{S,i})^{\boldsymbol{\nu}_i} = \frac{\Pi_i^{prod} (x_{S,i}\gamma_{S,i})^{\boldsymbol{\nu}_i}}{\Pi_i^{react} (x_{S,i}\gamma_{S,i})^{|\boldsymbol{\nu}_i|}} \tag{A4}$$

We can rewrite Eq. A-3 in terms of the following Damköhler number

$$Da = \frac{H_S k_f}{D + B} \tag{A5}$$

Substituting Eq. A4 and A5 into Eq. A3 gives

$$r = \frac{(D + B)\, Da}{H_S} \left(\prod_i^{react} x_{S,i}\gamma_{S,i} - \prod_i^{prod} x_{S,i}\gamma_{S,i} / K_{eq} \right) \tag{A6}$$

and the time-dependent material balance equations become

$$\frac{dH_S}{dt} = -D - B + E + \boldsymbol{\nu}_T (D + B) \times Da \left(\prod_i^{react} x_{S,i}\gamma_{S,i} - \prod_i^{prod} x_{S,i}\gamma_{S,i} / K_{eq} \right) \tag{A7}$$

$$H_S \frac{dx_{S,i}}{dt} = D(x_{S,i} - x_{D,i}) + B(x_{S,i} - x_{B,i}) - E(x_{S,i} - x_{E,i}) + (\boldsymbol{\nu}_i - \boldsymbol{\nu}_T x_{S,i})(D + B)Da\left(\prod_i^{react} x_{S,i}\gamma_{S,i} - \prod_i^{prod} x_{S,i}\gamma_{S,i}/K_{eq}\right) \quad \text{(A8)}$$

Finally, it should be noted that if a decanter is used at the top of the column, then x_D in these equations represents only the composition of the phase being removed as product.

Equality of projected upper and lower bounds at a pinch point

We are interested in looking at the projected upper and lower bounds because they tell us if column profiles can travel in feasible directions. The calculations are based on a pinch assumption which generally is not true; the projected upper bound is different from the projected lower bound as a result. It is of interest to confirm that the projected upper bound is equal to the projected lower bound at a true pinch point. That is, we wish to confirm that the following equation from Eq. 7 is true at a pinch point

$$\left(\frac{\tilde{V}_{n,POP}}{\tilde{E}_{POP}}\frac{\tilde{E}_{POP}}{\tilde{D}_{POP}} + \frac{\tilde{E}_{POP}}{\tilde{D}_{POP}} - 1\right) = \frac{\tilde{L}_{n,POP}}{\tilde{D}_{POP}} \quad \text{(A9)}$$

This will be proven by working backwards from this equation to known statements.

Inserting $\tilde{D}_{POP} = D[1 - x_{D,POP}]$, $\tilde{E}_{POP} = E[1 - x_{E,POP}]$, $\tilde{L}_{n,POP} = L_n[1 - x_{n,POP}]$, and $\tilde{V}_{n,POP} = V_n[1 - y_{n,POP}]$ to A-9 gives

$$\frac{V_n}{E}\frac{E}{D}\frac{[1 - y_{n,POP}]}{[1 - x_{D,POP}]} + \frac{E}{D}\frac{[1 - x_{E,POP}]}{[1 - x_{D,POP}]} - 1 = \frac{L_n}{D}\frac{[1 - x_{n,POP}]}{[1 - x_{D,POP}]} \quad \text{(A10)}$$

Multiply all terms by [1-$x_{D,POP}$] and rearranging this equation gives

$$\frac{V_n}{E}\frac{E}{D} + \frac{E}{D} - 1 - \frac{L_n}{D} = \frac{V_n}{E}\frac{E}{D}y_{n,POP} + \frac{E}{D}x_{E,POP} - x_{D,POP} - \frac{L_n}{D}x_{n,POP} \quad \text{(A11)}$$

Multiplying all terms by D, we get

$$V_n + E - D - L_n = V_n y_{n,POP} + E x_{E,POP} - D x_{D,POP} - L_n x_{n,POP} \quad \text{(A12)}$$

The expression on the left is the overall material balance and is zero at a pinch point. The expression on the right is a component-wise material balance and is also zero at a pinch point. Thus, both sides of the equation are zero, they are equal, and the starting equation is true.

Manuscript received May 20, 2005, and revision received Jan. 10, 2006.